

See discussions, stats, and author profiles for this publication at: <https://www.researchgate.net/publication/284233067>

# Fabric defect inspection using prior knowledge guided least squares regression

Article in *Multimedia Tools and Applications* · February 2017

DOI: 10.1007/s11042-015-3041-3

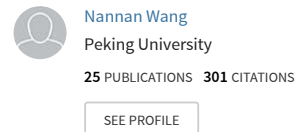
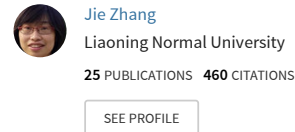
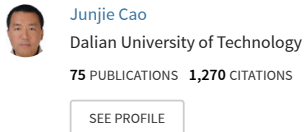
---

CITATIONS  
63

READS  
995

---

5 authors, including:



Some of the authors of this publication are also working on these related projects:



# Fabric Defect Inspection using Prior Knowledge Guided Least Squares Regression

Junjie Cao · Jie Zhang · Zhijie Wen\* · Nannan Wang · Xiuping Liu\*

Received: date / Accepted: date

**Abstract** This paper proposes an unsupervised model to inspect various defects in fabric images with diverse textures. A fabric image with defects is usually composed of a relatively consistent background texture and some sparse defects, which can be represented as a low-rank matrix plus a sparse matrix in a certain feature space. The process is formulated as a least squares regression based subspace segmentation model, which is convex, smooth and can be solved efficiently. A simple and effective prior is also learnt from local texture features of the image itself. Instead of considering only the feature space's global structure, the local prior is incorporated with it seamlessly by the proposed subspace segmentation model to guide and improve the segmentation. Experiments on a variety of fabric images demonstrate the effectiveness and robustness of the proposed method. Compared with existing methods, our method is more robust and locates various defects more precisely.

## 1 Introduction

Patterned fabric like wallpaper and ceramic, is a kind of typical texture image constructed from a repetitive pattern through a set of predefined symmetry rules. When the regularity is destroyed, different defects appear. Fabric defect inspection aims to detect and locate

Junjie Cao, Jie Zhang, Nannan Wang, Xiuping Liu  
School of Mathematical Sciences, Dalian University of Technology, Dalian, China  
E-mail: jjcao1231@gmail.com,  
xpliu@dlut.edu.cn(Corresponding author)

Zhijie Wen  
Department of Mathematics, College of Sciences, Shanghai University, Shanghai, China  
E-mail: wenzhijie@shu.edu.cn(Corresponding author)

these defects of patterned fabrics. It is a cornerstone in textile manufacturing. Traditionally, the inspection is mainly achieved by highly skilled and trained human inspectors. However, since the manual operations are easily influenced by subjective factors, such as human fatigue, it has a low detection rate only up to 70 percent [1]. Automated visual inspection [2, 3] improves such inspection and attracts substantial attention in recent decades.

The existing automated defect inspection techniques are basically divided into three categories: model-based, statistical and spectral approaches. Model-based paradigms [4, 5] identify defects via modeling defect-free textures. Their results tend to be unsatisfying and they usually share a high computational complexity. Spectral approaches [6–9] extract defects by transforming fabric images to the spectrum domain, and their performance hinges on the chosen filter to a great degree. Statistical approaches [10–12], using diverse statistical properties of textures and defects, may effectively detect fabric defects. But the texture pattern and defect shape have a crucial influence on the detection results of statistical and spectral approaches, such as [12, 13], see Fig.1. Some recently technologies [14, 15] do not have the problem. However some fake defects may be detected and they fail to locate defects precisely, see Fig.2.

In order to handle these problems, we propose a novel and robust approach for the fabric defect inspection utilizing the structure of the image's feature space. The approach is inspired by the recently proposed low-rank representation (LRR). Since defect-free regions of a fabric image are consisted of repeated patterns, texture features of those regions are similar *i.e.*, they are in a low-rank subspace. Whereas, features of defective regions tend to destroy the regularity and are usually far away from the subspace spanned by those of the defect-

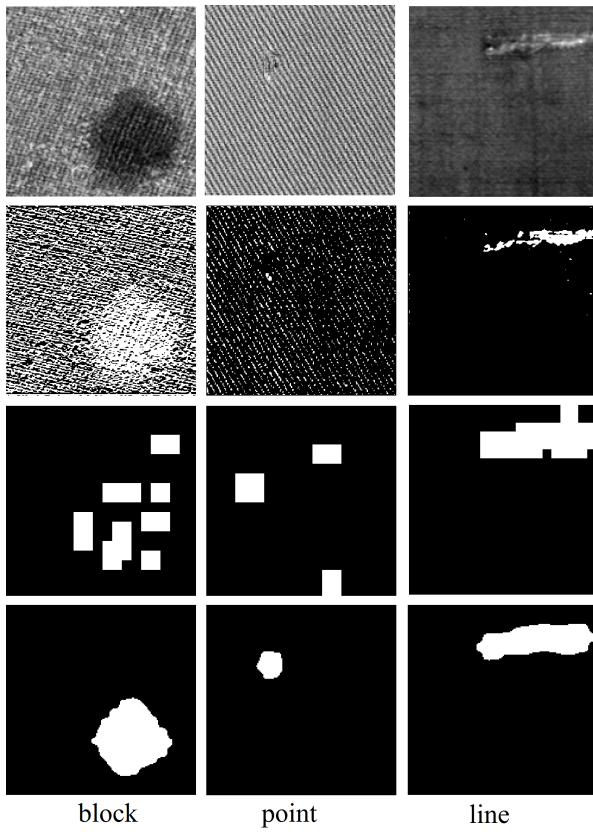


**Fig. 1** Our method is more robust for different background textures and defect shapes. The original images, detection results of AW, MLBp, and our method are listed from top to bottom.

free regions. LRR can capture the subspace structure even if the features are contaminated by outliers. However, it considers only the global structure of the data's feature space, and it is time-consuming. To further improve the inspection results and reduce the running time, we propose prior knowledge guided least squares regression (PG-LSR). It is a variation of LRR with continuous and differentiable objective function, hence it is easier to be solved and takes less running time. A simple and effective method is designed to learn the prior knowledge from randomly sampled local texture features of the input fabric image itself. PG-LSR generates more faithful results by incorporating the local prior with the global structure. We summarize the contributions of this paper as follows:

- PG-LSR is proposed for general subspace segmentation problem. It recovers the subspace structure as well as LRR but with less running time. The prior knowledge can be obtained by many ways for different applications to improve the segmentation.
- For fabric defect inspection, a simple and efficient unsupervised learning process is designed to esti-

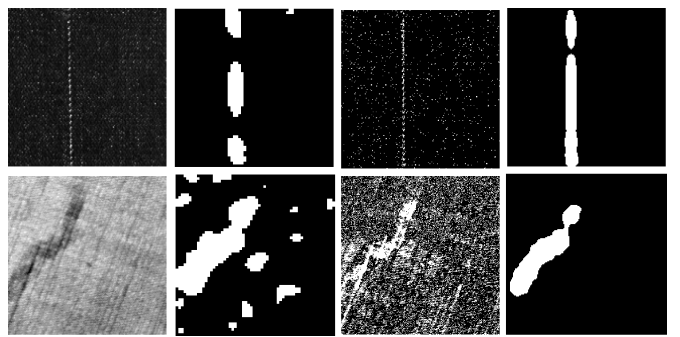


**Fig. 2** Our method locates the defective regions accurately. The original images, the detection results of SR, RRSVD, and our method are listed from left to right.

mate the prior knowledge from local texture features of the input fabric image itself. The prior knowledge are integrated with the global structure of the texture feature space via RG-LRS to identify various defects accurately and robustly.

## 2 Related work

### 2.1 Fabric defect detection

Defect detection plays an important role in fabric quality control process. There has been a considerable mount of works on it. The existing defect detection techniques are basically divided into three categories: model-based, spectral and statistical approaches.

The model-based methods extract image texture features through modelling and parameter estimation techniques. Hajimowlana et al. [16] introduce the 1D autoregressive method to defect detection. Ozdemir et al. [17] employ the Markov random field model to detect the defects on fabric images. Cohen et al. [18] suggest applying Gaussian Markov random field to model defect-free textures of fabric images. Recently, a wavelet-domain hidden Markov tree model combining with the level set segmentation technique is proposed by Chan et al. [19]. However, the detection results of these methods are not very satisfying and they usually share a high computational complexity.

In spectral approaches, the fabric images are first transformed into the spectrum domain and then the features are extracted by some energy criterion. These transformations include Fourier transform [6], wavelet transform [7, 13, 20–22], Gabor transform [8, 23] and other filtering methods [9, 24]. However, the pattern and defect shape of the fabric image have a significant influence on their performance [25].

Statistical approaches employ the spatial distribution of gray values of texture features for fabric defects detection. Tsai et al. [10] and Wood [26] use the co-occurrence matrix and auto-correlation of sub-images to extract the texture features, respectively. Zhang et al. [11] exploit the mean and standard deviations of sub-blocks to describe the distribution. A variant of local binary patterns (LBP) is designed by Tajeripour et al. [12] to detect fabric defects. More recently, a graph on image manifold is used to describe the distribution of images [27]. However, similar with spectral approaches, the results of different statistic approaches are often specific to texture patterns and defect shapes. In this paper, the proposed method copes with various textures and defects.

Recently, there are also some technologies focusing on the problem. Chetverikov et al. [15] treat the fabric image as a matrix which is constructed by a periodic signal and detect the defects by Singular Value Decomposition (SVD). Fabric defect detection can also be modeled as saliency detection. Ann and Kim [14] detect the defects by the difference between the original signal and a smooth one in the log amplitude spectrum. However, these methods often generate some fake detections. Our method locates the defects accurately.

## 2.2 Saliency detection based on low-rank representation

Saliency detection is an important and active topic in computer vision, due to its applications to object detection [28] and image editing [29, 30]. Given a natural image, the goal of it is to find the salient areas from complex scenes. In a fabric image, the defective regions can be regarded as the salient areas. Therefore, some methods based on saliency detection are proposed to detect defects in fabric images, such as [14]. LRR achieves excellent performance in motion segmentation, image segmentation and saliency detection [31–35]. Based on LRR, Lang et al. [35] formulate the saliency detection process as a constrained nuclear norm and  $l_{2,1}$ -norm minimization problem. This method achieves excellent performance in saliency detection. However, there exist two problems when apply it to fabric defect detection. First, it is time-consuming to solve the objective function. Yu et al. [36] and Lu et al. [37] theoretically show that similar results can be obtained with far less runtime, if the nuclear norm and  $l_{2,1}$ -norm are replaced by  $F$ -norm. Second, and more importantly, the method proposed in [35] does not perform well on fabric images since it is designed to handle natural images. For the fabric defect detection, we choose an effective texture feature to replace the multiple features used in [35].

Moreover, utilizing the the texture feature, a simple and effective prior knowledge is learnt from the input image itself to improve the detection results further.

## 3 Algorithm

With a defective fabric image as input, our algorithm takes three steps to detect the defective regions. First, we partition the input image into blocks (superpixels) and extract a feature vector for each block (see section 3.1). Then we use PG-LSR to obtain an irregularity map, where higher values indicate higher probability to be defective. Finally, the defective regions are obtained though automatic thresholding. The two steps are described in section 3.2. In order to couple the prior about local contrast with the feature space's global structure, a guiding matrix is employed in PG-LSR. Aiming at identifying fabric defects, we design an effective unsupervised process to construct the guiding matrix (see section 3.3).

### 3.1 Image partition and feature extraction

The given image  $\mathbf{I}$  is divided into blocks with size  $m \times m$  pixels. For each block  $\mathbf{B}_i$ , a feature vector  $\mathbf{x}_i$  is extracted to describe the structure of it. Specifically, we compute a 8-D texture feature [38]  $\mathbf{t}_j$  for each pixel  $p_j$  of the image  $\mathbf{I}$  and define the feature vector for the block  $\mathbf{B}_i$  as:

$$\mathbf{x}_i = \frac{1}{|\mathbf{B}_i|} \sum_{p_j \in \mathbf{B}_i} \mathbf{t}_j, \quad (1)$$

where  $|\mathbf{B}_i|$  is the cardinality of set  $\mathbf{B}_i$ . Let  $\mathbf{X} = [\mathbf{x}_1, \mathbf{x}_2, \dots, \mathbf{x}_N] \in \mathbb{R}^{8 \times N}$  be the feature matrix, where  $N$  is the total number of blocks.

### 3.2 Fabric defect detection

#### 3.2.1 Locating defective regions by LRR

There usually exists strong correlation among the feature vectors of defect-free background blocks, whereas the defective regions hanging over the repeated patterns are different from the background blocks. Therefore, the feature matrix could be decomposed into a defect-free part and a defective part by LRR:

$$\min_{\mathbf{Z}, \mathbf{E}} \|\mathbf{Z}\|_* + \lambda \|\mathbf{E}\|_{2,1} \quad s.t. \mathbf{X} = \mathbf{XZ} + \mathbf{E}, \quad (2)$$

where  $\|\cdot\|_*$  denotes the matrix nuclear norm, the parameter  $\lambda > 0$  is used to balance the effects of two

parts, and  $\|\cdot\|_{2,1}$  is the  $\ell_{2,1}$ -norm defined as the sum of  $\ell_2$  norms of the columns of a matrix.

The feature matrix  $\mathbf{X}$  is reconstructed by itself plus some errors encoded by the matrix  $\mathbf{E}$ . The matrix  $\mathbf{Z}$  denoting the reconstruction coefficients should have the property of low-rankness. The nuclear norm of  $\mathbf{Z}$  is a convex relaxation of the rank function. The matrix  $\mathbf{E}$  standing for the defective part should be sparse because the defective regions only account for a very small fraction of a fabric image. The minimization of  $\ell_{2,1}$ -norm encourages the columns of  $\mathbf{E}$  to be zero, which fits the defect detection problem well.

We define the irregularity map  $S$  by the optimal solution  $\mathbf{E}^*$  (with respect to  $\mathbf{E}$ ) of problem (2):

$$S(\mathbf{B}_i) = \|\mathbf{E}^*(\cdot, i)\|_2^2 = \sum_j (\mathbf{E}^*(j, i))^2, \quad (3)$$

where  $\mathbf{E}^*(\cdot, i)$  and  $\mathbf{E}^*(j, i)$  are the  $i$ -th column and  $(j, i)$ -th entry of matrix  $\mathbf{E}^*$ , respectively. The large score of  $S(\mathbf{B}_i)$  means that the block  $\mathbf{B}_i$  has high probability to be defective. The irregularity value of pixel  $p_i$  is defined as the sum of irregularity values of the blocks which cover the pixel. The second column of Figure 3 illustrates the irregularity maps obtained by LRR for some fabric images. The results show that LRR can locate the defects, although there is some interference.

### 3.2.2 Improving the detection results by PG-LSR

Although LRR can roughly identify the defects, the matrix nuclear norm is not smooth. The popular method used to solve the equation (2) is Augmented Lagrange Multiplier (ALM) method [39] which computes the singular value decomposition (SVD) of a  $N \times N$  matrix in each iteration. That is a time-consuming process.  $F$ -norm, which is easy to solve, can be used to replace the nuclear norm and  $\ell_{2,1}$ -norm in equation (2):

$$\min_{\mathbf{Z}, \mathbf{E}} \|\mathbf{Z}\|_F^2 + \lambda \|\mathbf{E}\|_F^2 \quad s.t. \mathbf{X} = \mathbf{XZ} + \mathbf{E}, \quad (4)$$

where  $\|\mathbf{A}\|_F^2 = \sum_{i,j} (\mathbf{A}(i, j))^2$ ,  $\mathbf{A} \in \mathbb{R}^{N \times N}$ . This model is called least squares regression (LRS). The third column of Figure 3 is the irregularity maps obtained by LRS, which performs a little worse than LRR. But the running time of solving Equation (4) is just a quarter of the time for solving Equation (2).

To get a clear irregularity map, we propose prior knowledge guided least squares regression (PG-LSR):

$$\min_{\mathbf{Z}, \mathbf{E}} \|\mathbf{Z}\|_F + \lambda \|\mathbf{EW}\|_F \quad s.t. \mathbf{X} = \mathbf{XZ}_0 + \mathbf{E}_0, \quad (5)$$

where the guiding matrix  $\mathbf{W} \in \mathbb{R}^{N \times N}$  is diagonal. We resort to the matrix  $\mathbf{W}$  to guide the defective part  $\mathbf{E}$

by suppressing the defect-free region. Therefore a large value is set to  $\mathbf{W}(i, i)$  when block  $\mathbf{B}_i$  is considered as a defect-free region. We design a effective method to construct  $\mathbf{W}$  which is described in section 3.3. Benefiting by the guiding item, the irregularity maps obtained by PG-LSR are more clear and accurate (see the fifth column of Figure 3).

To make the irregularity map defined on the pixel level more smooth, a Gaussian filtering is performed. The defective regions are obtained though simple threshold segmentation. Specifically, we use the Otsus method to choose a threshold automatically and the pixel  $p_i$  is regarded as defective if its irregularity value is larger than the threshold.

### 3.3 Construction of the guiding matrix

In order to construct the guiding matrix  $\mathbf{W}$ , we first compute a reference feature vector  $\mathbf{m}$  which is considered as a typical feature for the defect-free regions. Since the defective regions usually account for a very small fraction of the entire image, a randomly-chosen image block has a very high probability to be defect-free. We randomly choose  $s$  blocks from the image and use the mean feature vectors of these blocks as a candidate reference feature vector. This process is repeated  $k$  times. Therefore there are  $k$  candidate reference feature vectors, which are denoted by  $\mathbf{m}_1, \mathbf{m}_2, \dots, \mathbf{m}_k$ . The reference feature vector  $\mathbf{m}$  is defined as the optimal solution of the following problem:

$$\mathbf{m} = \arg \min_{\mathbf{m}} \sum_i \|\mathbf{m}_i - \mathbf{m}\|_1, \quad (6)$$

where  $\|\cdot\|_1$  is the  $L_1$  norm.

For each block  $\mathbf{B}_i$ , the distance between feature vector  $\mathbf{x}_i$  and reference feature vector  $\mathbf{m}$  is used to construct the prior knowledge, i.e.,  $P_i = \|\mathbf{x}_i - \mathbf{m}\|_2^2$ . Since the large value of prior knowledge  $P_i$  means the high score of block  $\mathbf{B}_i$  to be a defective region, the weight  $\mathbf{W}(i, i)$  corresponding to block  $\mathbf{B}_i$  is defined as:

$$\mathbf{W}(i, i) = \exp(-P_i). \quad (7)$$

The fourth and fifth columns of Figure 3 show the irregularity maps obtained by the prior knowledge and PG-LSR, respectively. From the results we can find that PG-LSR generate perfect maps, even when the prior knowledge includes much noise.

## 4 Experimental results

We have shown that our method is robust to different texture patterns and defect shapes, and locates defects

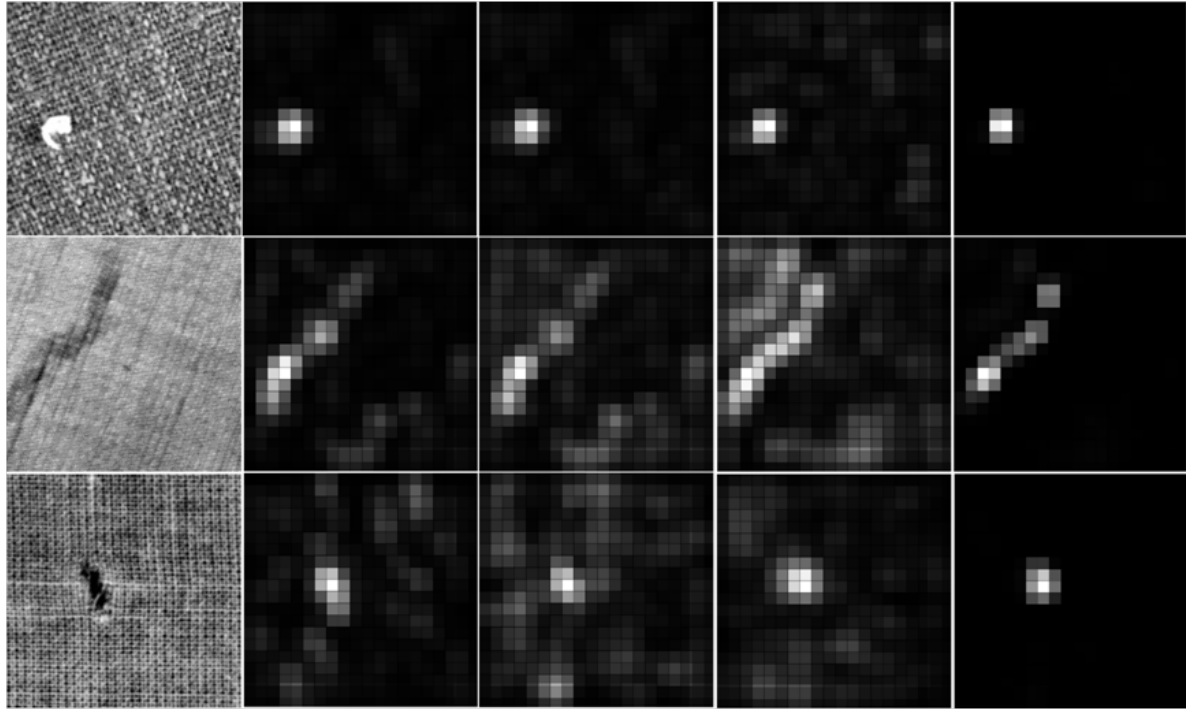


**Fig. 3** Comparison of irregularity maps. The original images, the irregularity maps obtained by LRR, LRS, Prior knowledge, and PG-LSR are listed from left to right.

more precisely in Fig.1 and 2. To evaluate our method more thoroughly, more comparisons are examined in section 4.1. Section 4.2 and 4.3 present that our method is insensitive to parameters and robust to noise.

The test images used in this section are obtained from TILDA Textile Texture Database or a production line. All the images have the size  $256 \times 256$ . To show the advantages of our method, we implement four previous methods for comparison, which are residual of resonant SVD (RRSVD) [15], adaptive wavelets (AW) [13], spectral residual (SR) [14, 25], and modified local binary patterns (MLBP) [12].

We divide input images into overlapping blocks. The size of block is  $16 \times 16$  and the overlapping step is 8. The parameters  $\lambda$ ,  $s$  and  $k$  of our method are chosen as  $\lambda = 0.75$ ,  $s = 5$ ,  $k = 5$  for all the experiments.

#### 4.1 Comparison with other methods

##### 4.1.1 Simple plain and twill fabric images

**Comparison of irregularity maps.** Given a fabric image, defect detection algorithms tend to generate an irregularity map first. Then the defects are located by thresholding. The irregularity maps obtained by AW, RRSVD, MLBP, SR, and our method are shown in Figure 4.

Compared with AW: The irregularity maps obtained by AW can recognize most defective regions. However, the contrast of the irregularity maps is low, especially for large block shaped defects, as shown in the eighth and ninth rows of Figure 4. It is difficult to define a proper threshold to locate the defects.

Compared with RRSVD: RRSVD extracts defects directly from the difference between the original image and periodic pattern. Many fake defects tend to be generated when the fabric images contain noise, fickle shadows and illumination changes, which lead to very noisy irregularity maps.

Compared with MLBP: MLBP employs the local binary pattern to detect the defective regions. Since this feature is gray scale invariant, MLBP fails to identify defects when the defective and defect-free regions share consistent texture but different colors, see the last two rows of Figure 4 for details.

Compared with SR: The irregularity maps obtained by SR are not able to recognize the defective regions which are large and smooth, such as the last three rows of Figure 4.

Our method: Compared with other methods, the irregularity maps generated by our method are more accurate and clear. To obtain satisfied detection results, delicate thresholding methods, even manually adjusted thresholds, are necessary for RRSVD, AW and SR to extract

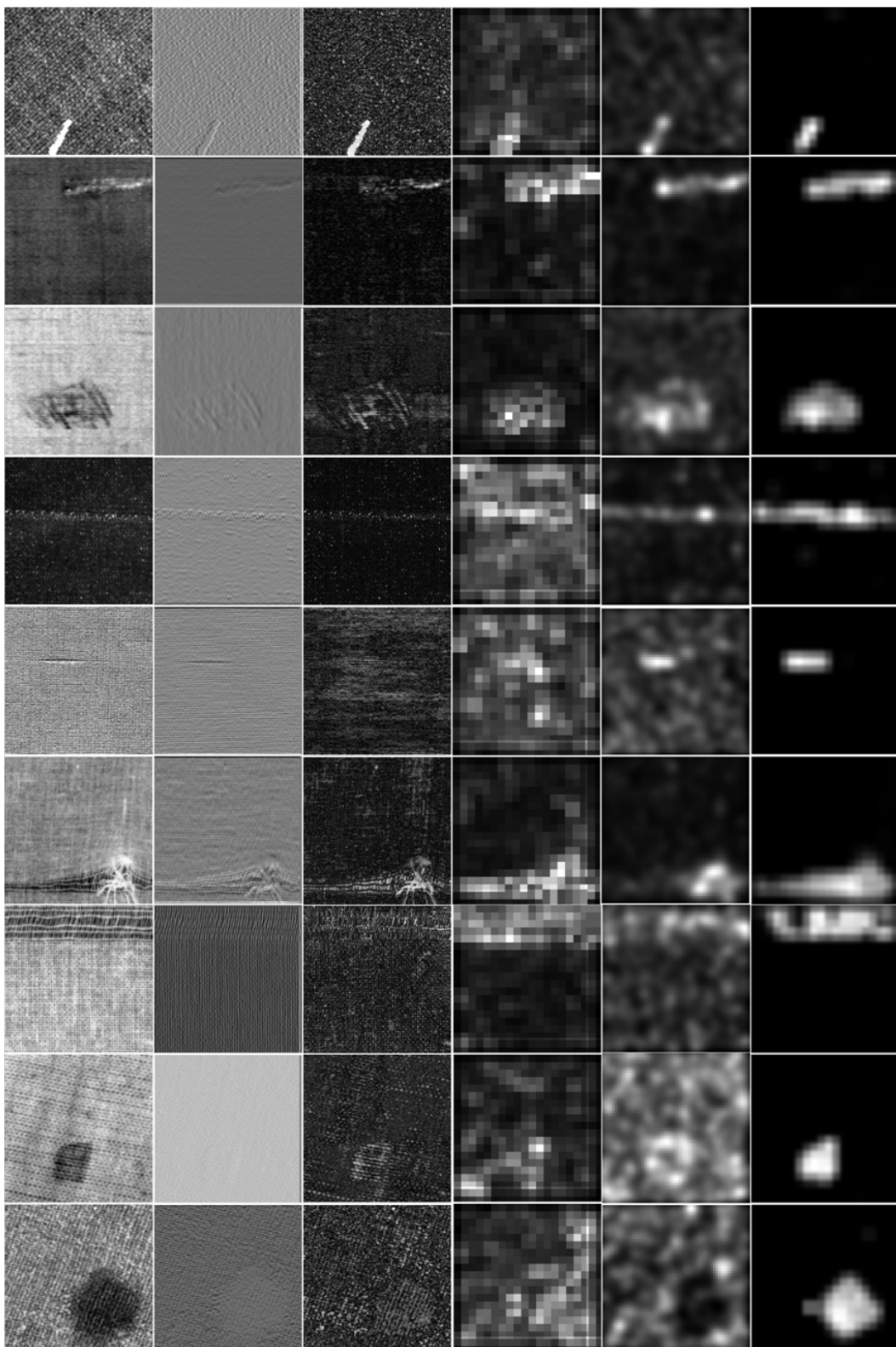


**Fig. 4** Comparison of irregularity maps. The first column is the original images. The irregularity maps of AW, RRSVD, MLBP, SR and our method are listed from the second column to the last.

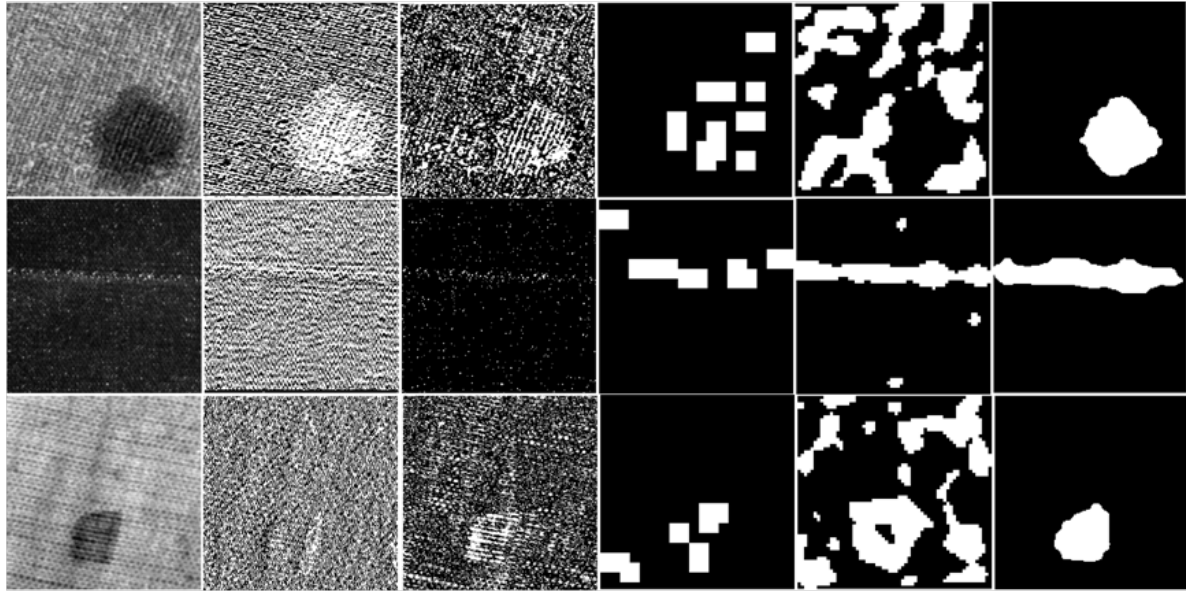


**Fig. 5** Comparison of detection results. The first column is the original images. Detection results of AW, RRSVD, MLBP, SR and our method are listed from the second column to the last.

defects from the irregularity maps. However, the irregularity maps of our method are so clear that automatic thresholding is enough. Moreover, all the other methods tend to fail when the defective regions are small and the contrast between them and defect-free regions is low, as shown in the fifth row of Figure 4. Our method handles such defects well.

**Comparison of detection results.** Figure 5 shows the detection results of AW, RRSVD, MLBP, SR and our method. All of these methods do not provide the way to choose a proper threshold except MLBP. For RRSVD, AW, SR, and our method, we use the Otsu's method to choose the threshold automatically. This method chooses the threshold to minimize the intraclass variance of the black and white pixels. The threshold for MLBP is selected based on the training image, as described in the paper [12]. We choose a piece of defect-free region in the test image manually and take the chosen region as the training image. As shown in Figure 4, the irregularity maps obtained by AW, RRSVD, SR and MLBP are ambiguous and include some false and misleading information. Hence, there are some missing defects and fake defects in their final detection results, see Figure 5. Since the irregularity maps of our method are clear, we locate the defects accurately.

#### 4.1.2 More complicated patterns

Previous methods, such as AW, Fourier transform [6] and Gabor transform [23], mostly focus on detecting defective objects in simple plain and twill fabric im-

ages. Our method can detect the defective regions accurately even for the images with more complicated patterns. Figure 6 shows the irregularity maps of RRSVD, MLBP, SR and our method for the box- and star-patterned images. As expected, the irregularity maps of our method are more clear and the locations of the defective regions are more accurate.

#### 4.2 Parameter insensitivity

Four key parameters in our method are  $\lambda$ ,  $s$ ,  $k$ , and the size of block.  $\lambda$  is the trade-off parameter in Equation (5). The irregularity maps with different parameters are shown in Figure 9. From the results we can see that the proposed PG-LSR model works well under a large range of parameter settings. The irregularity maps are almost invariant when the parameter ranges from 0.25 to 1.25.  $s$  and  $k$  are two parameters used to construct the reference feature vector. We change the values of  $s$  and  $k$  between 3 and 15, and compute the distances between each pair of reference feature vectors obtained by them (see Figure 7). The experiments show that these reference feature vectors vary little with  $s$  and  $k$ . Specifically, the Euclidean distances and angles between these vectors vary from 0 to 0.08. Figure 8 shows the irregularity maps obtained by different sizes of block. When the block size is small, our method describes the shapes of the defective regions better. But the texture features are also more easily influenced by noise, such as fickle shadows and illumination changes. Therefore the irreg-

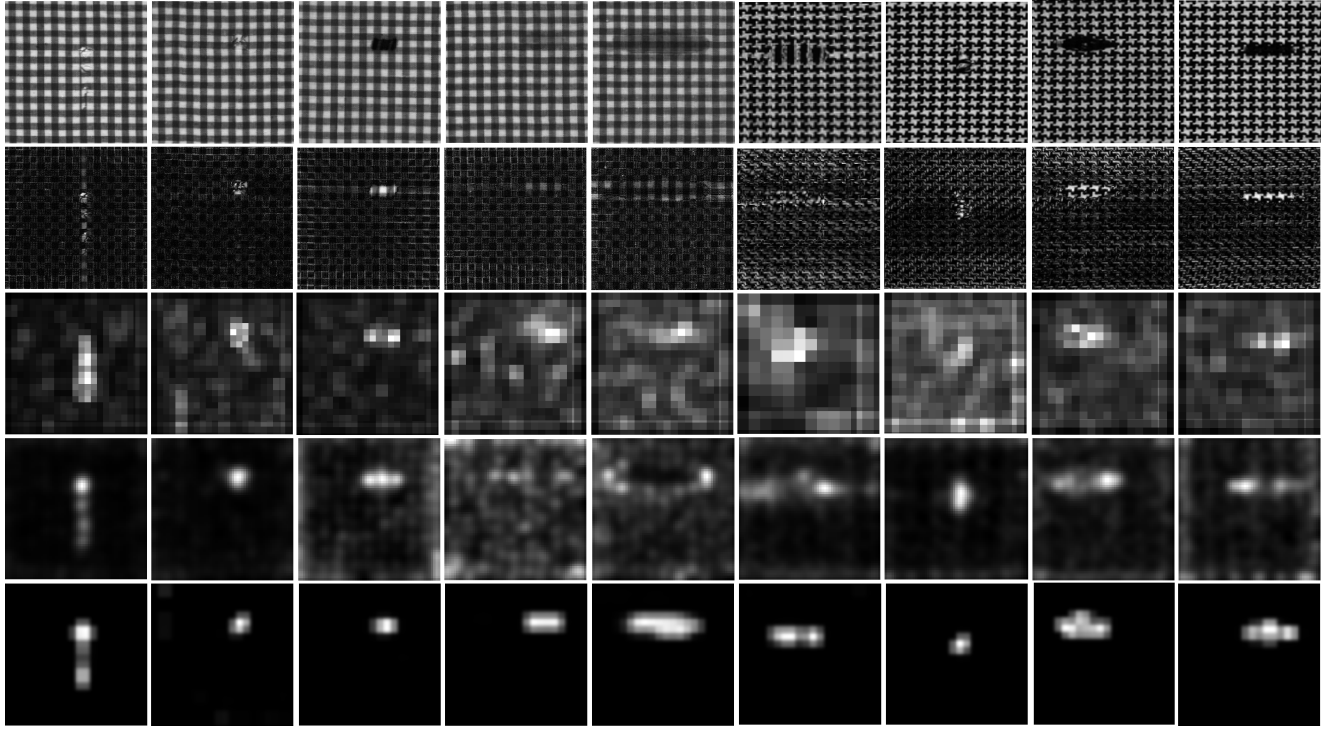


**Fig. 6** Comparison of irregularity maps for the fabric images with more complicated pattern. The first row is the original images. Detection results of RRSVD, MLBP, SR and our method are listed from the second row to the last.

ularity maps may contain some small noise, as shown in the last row of Figure 8. To make a compromise, we set the size of block as  $16 \times 16$  in our experiments.

#### 4.3 Robustness

In order to demonstrate the robustness of our method, the centered Gaussian noise are added in the test images. Figure 10 and Figure 11 show the irregularity maps of images which are perturbed by centered Gaussian noise with the standard deviation of 0.02, 0.04 and 0.06. From the results we can see that the irregularity maps of AW, RRSVD, and WLBP are severely affected by the noise. Our method and SR generate more stable irregularity maps since both of them take usage of the global structure of the fabric images. But the results of our method are much clearer than those of SR, especially when the noise is large, as shown in the third and fourth rows of Figure 10 and 11.

## 5 Conclusion

In this paper, a novel and robust fabric defect inspection method is proposed. We use PG-LSR to combine the global structure of texture feature space and the

prior from local similarity seamlessly. This combination helps to generate a more clear irregularity map and improve robustness of the proposed method. The experimental results show that our method can inspect various fabric defects in spite of diverse background texture patterns. Compared with other methods, it locates the defect more precisely. Also, it is robust to noise and different parameters.

There is a limitation of our method as we can see from the experimental results. The identified defects are blocky since the tested image is divided into blocks first, which leads to inaccurate shape description of the defect. Future work may focus on accurate depiction of the defects' shape and automated fabric defect classification after the detection.

## Acknowledgement

The authors would like to thank Huanhuan Zhang for her images of TILDA Textile Texture Database. Junjie Cao is supported by the NSFC China (61363048, 91230103). Zhijie Wen is supported by the NSFC China (11471208). Xiuping Liu is supported by the NSFC China (61173102, 61370143).

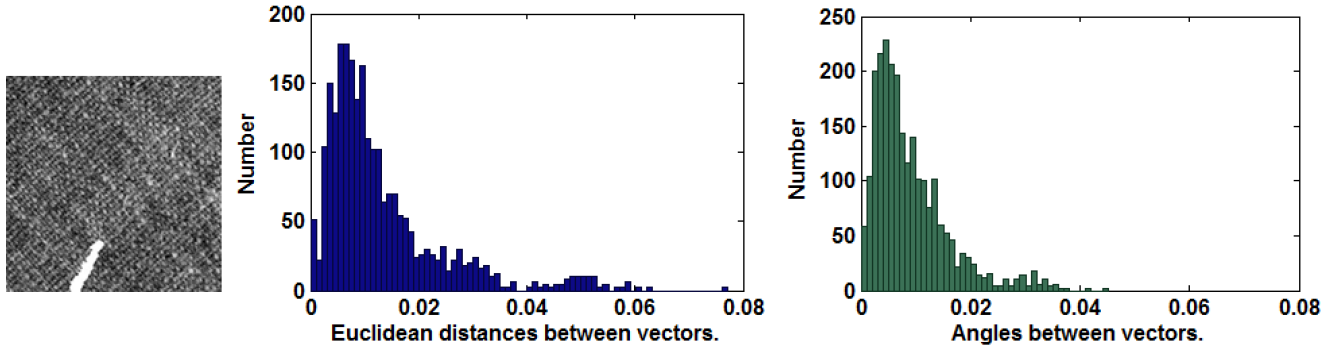


**Fig. 7** The distribution of distances and angles between each pair of reference feature vectors obtained by different  $s$  and  $k$ . The first column is a fabric image. The second and third columns show the distributions of Euclidean distances and angles between the image's reference feature vectors obtained by different  $s$  and  $k$ , respectively. Here  $s, k \in \{3, 5, 7, 11, 13, 15\}$ .

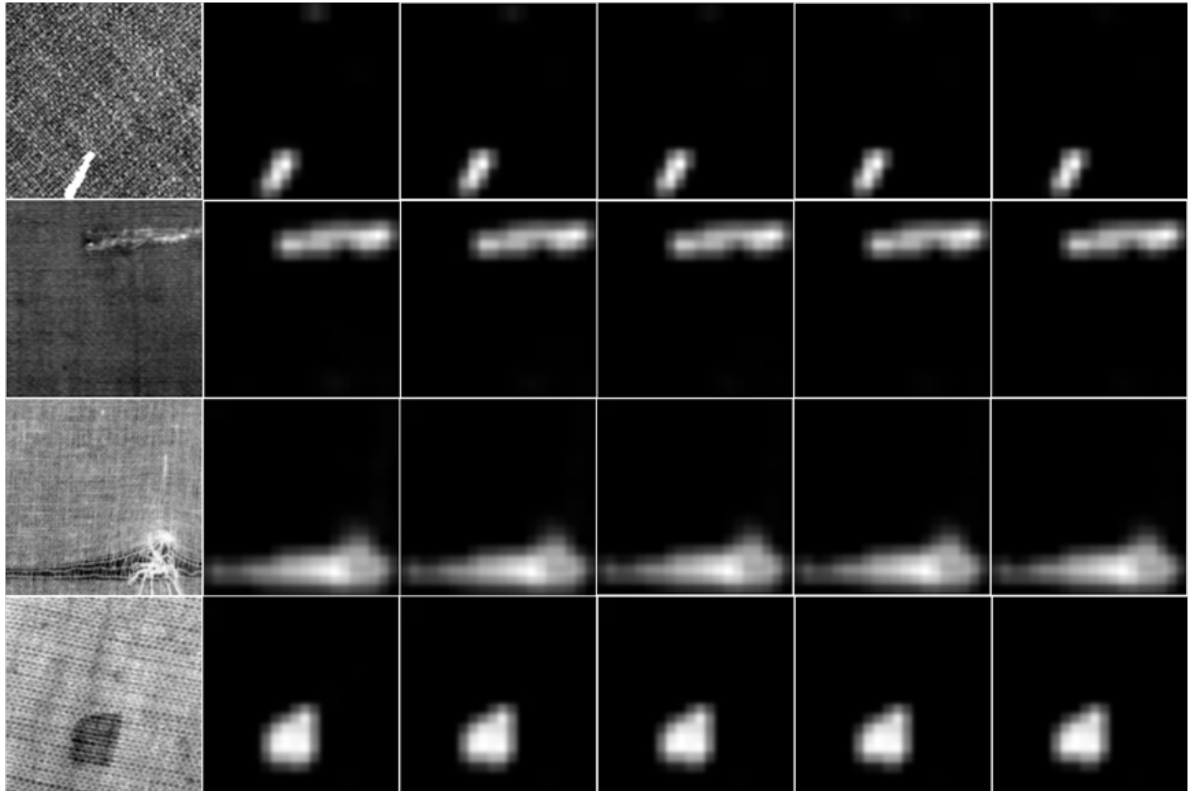


**Fig. 9** In sensitive to parameter  $\lambda$ . The first column is the original images. Detection results by set  $\lambda = 0.25, 0.5, 0.75, 1.0, 1.25$  are listed from the second column to the last.

## References

1. K. L. Mak and P. Peng, "An automated inspection system for textile fabrics based on gabor filters," *Robotics and Computer-Integrated Manufacturing*, vol. 24, no. 3, pp. 359–369, 2008.
2. R. T. Chin and C. A. Harlow, "Automated visual inspection: A survey," *IEEE Transactions on Pattern Analysis and Machine Intelligence*, vol. 4, no. 6, pp. 557–573, 1982.
3. H. Y. T. Ngan, G. K. H. Pang, and N. H. C. Yung, "Automated fabric defect detection - a review," *Image and Vision Computing*, vol. 29, no. 7, pp. 442–458, 2011.
4. F. S. Cohen, Z. Fan, and S. Attali, "Automated inspection of textile fabrics using textural models," *IEEE Transactions on Pattern Analysis and Machine Intelligence*, vol. 13, no. 8, pp. 803–808, 1991.
5. O. Alata and C. Ramananjarasoa, "Unsupervised textured image segmentation using 2-d quarter plane autoregressive model with four prediction supports," *Pattern Recognition Letters*, vol. 26, no. 8, pp. 1069–1081, 2005.
6. C. H. Chan and G. K. H. Pang, "Fabric defect detection by fourier analysis," *IEEE Transactions on Industry Applications*, vol. 36, no. 5, pp. 1267–1276, 2000.

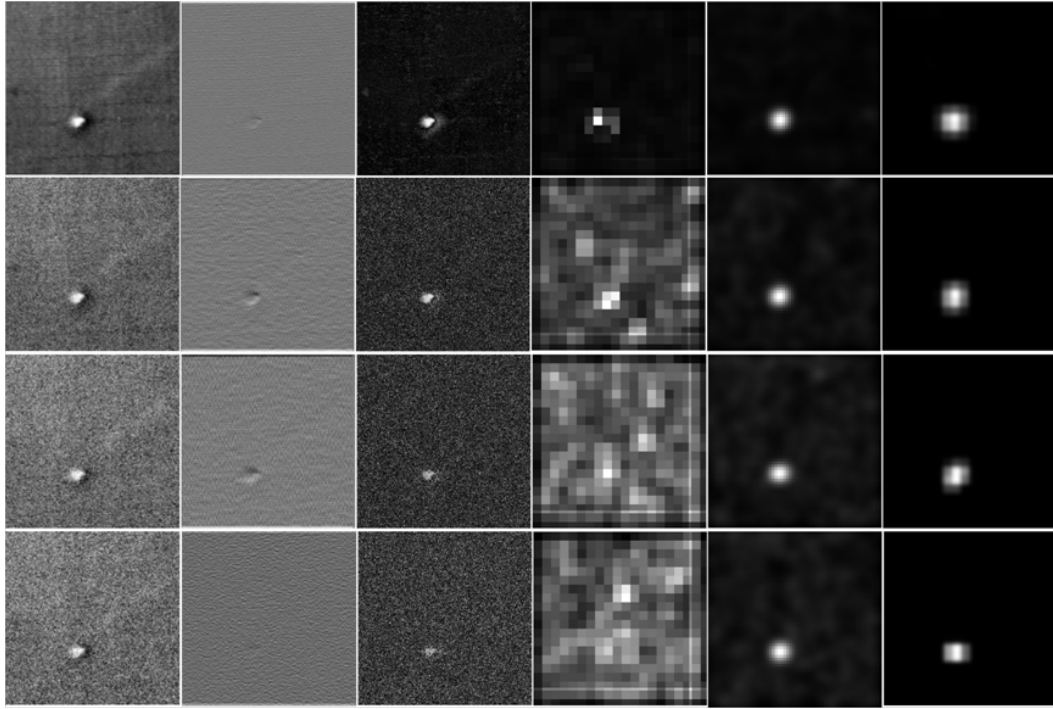


**Fig. 10** Robust to noise. The input image, detection results of AW, RRSVD, MLBP, SR and our method are listed from left to right. The top row is the noise-free image. The deviation of Gaussian noise for the second, third and fourth rows are 0.02, 0.04 and 0.06, respectively.

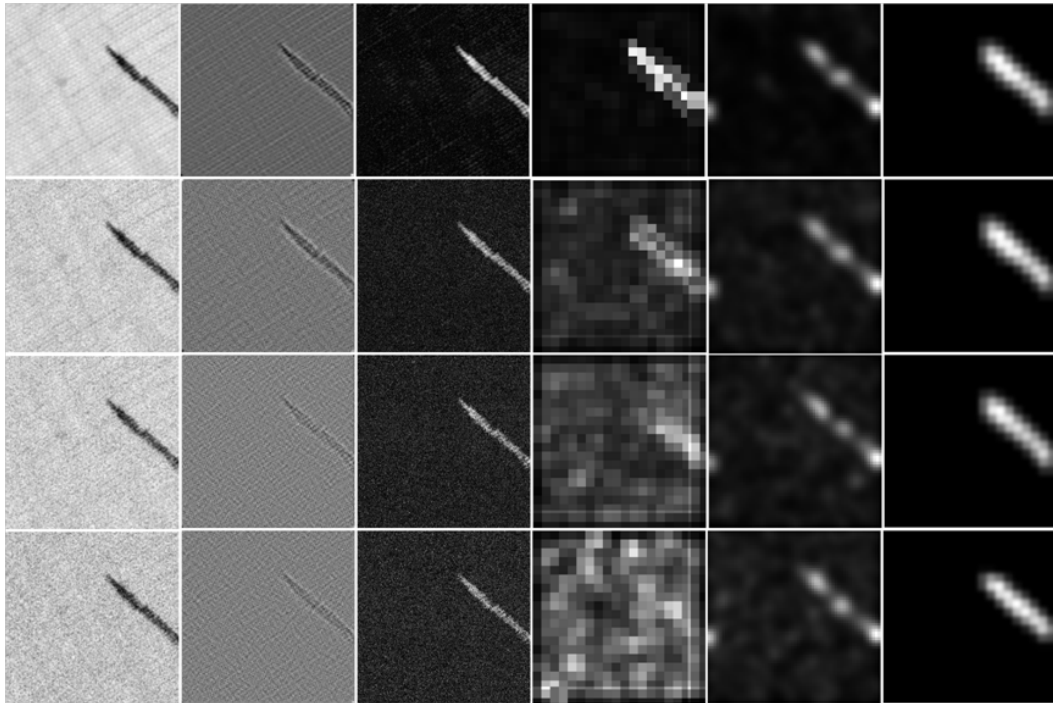


**Fig. 11** Robust to noise. The input image, detection results of AW, RRSVD, MLBP, SR and our method are listed from left to right. The top row is the noise-free image. The deviation of Gaussian noise for the second, third and fourth rows are 0.02, 0.04 and 0.06, respectively.

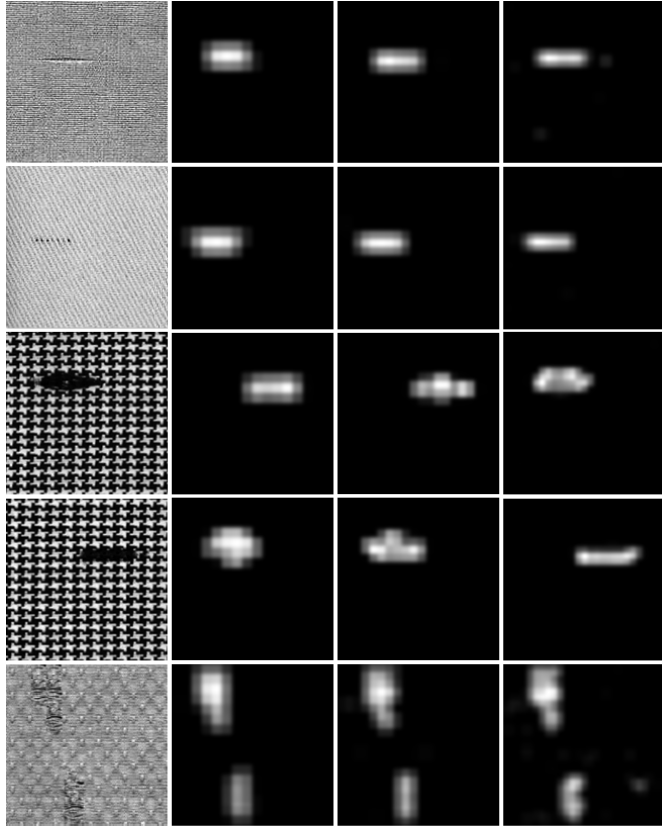


**Fig. 8** The irregularity maps of our method with different size of block. The first column is the original images. From the second column to the last, the size of block is  $20 \times 20$ ,  $16 \times 16$ , and  $12 \times 12$ , respectively.

7. X. Yang, G. Pang, and N. Yung, "Robust fabric defect detection and classification using multiple adaptive wavelets," *IEE Proceedings - Vision, Image and Signal Processing*, vol. 152, no. 6, pp. 715–723, 2005.
8. N. Ogata, S. Fukuma, H. Nishikado, A. Shiroasaki, S. Takagi, and T. Sakurai, "An accurate inspection of pdp-mesh cloth using gabor filter," in *Proceedings of International Symposium on Intelligent Signal Processing and Communication Systems. ISPACS 2005*. Hongkong: IEEE, Dec 2005, pp. 65–68.
9. A. Kumar and G. K. H. Pang, "Defect detection in textured materials using optimized filters," *IEEE TRANSACTIONS on SYSTEMS Man and Cybernetics PART b-cybernetics*, vol. 32, no. 5, pp. 553–570, 2002.
10. I. Tsai, C. Lin, and J. Lin, "Applying an artificial neural network to pattern recognition in fabric defects," *Textile Research Journal*, vol. 65, no. 3, pp. 123–130, 1995.
11. X. F. Zhang and R. R. Bressee, "Fabric defect detection and classification using image analysis," *Textile Research Journal*, vol. 60, no. 4, pp. 1–9, 1995.
12. F. Tajeripour, E. Kabir, and A. Sheikhi, "Fabric defect detection using modified local binary patterns," in *International Conference on Computational Intelligence and Multimedia Applications*, 2008, pp. 261–267.
13. Z. Wen, J. Cao, X. Ping, and S. Hui, "Fabric defects detection using adaptive wavelets," *International Journal of Clothing Science and Technology*, vol. 26, no. 3, pp. 202–211, 2014.
14. I. Ahn and C. Kim, "Finding defects in regular-texture images," in *Korea-Japan Joint Workshop on Frontiers of Computer Vision*, 2010.
15. D. Chetverikov, "Residual of resonant SVD as salient feature," in *International Conference on Computer Vision and Graphics, ICCVG 2008*, Warsaw, Poland, November 2008, pp. 143–153.
16. S. H. Hajimowlana, R. Muscedere, G. A. Jullien, and J. W. Roberts, "1D autoregressive modeling for defect detection in web inspection systems," in *Midwest Symposium on Circuits and Systems*, 1998, pp. 318–321.
17. S. Ozdemir and A. Ercil, "Markov random fields and Karhunen-Loeve transforms for defect inspection of textile products," in *IEEE Conference on Emerging Technologies and Factory Automation, EFTA 1996*, 1996, pp. 697–703.
18. F. S. Cohen, Z. Fan, and S. Attali, "Automated Inspection of Textile Fabrics Using Textural Models," *IEEE Transactions on Pattern Analysis and Machine Intelligence*, vol. 13, pp. 803–808, 1991.
19. H.-Y. Chan, C. Raju, H. Sari-Sarraf, and E. F. Hequet, "A general approach to defect detection in textured materials using a wavelet domain model and level sets," in *Proceeding SPIE, Vol. 6001*, 2005, pp. 102–107.
20. Y. X. Zhi, G. K. H. Pang, and N. H. C. Yung, "Fabric defect detection using adaptive wavelet," in *IEEE International Conference on Acoustics, Speech, and Signal Processing*, 2001, 2001, pp. 3697–3700.
21. X. Yang, G. Pang, and N. Yung, "Discriminative training approaches to fabric defect classification based on wavelet transform," *Pattern Recognition*, vol. 37, no. 5, pp. 889–899, 2004.
22. H. Y. T. Ngan, G. K. H. Pang, S. P. Yung, and M. K. Ng, "Wavelet based methods on patterned fabric defect detection," *Pattern Recognition*, vol. 38, no. 4, pp. 559–576, 2005.
23. A. Kumar and G. K. H. Pang, "Defect detection in textured materials using gabor filters," *IEEE Transactions on Industry Applications*, vol. 38, no. 2, pp. 425–440, 2002.
24. P. Zeng and T. Hirata, "On-loom fabric inspection using multi-scale differentiation filtering," in *IEEE 37th IAS Industry Applications Conference Meetings*, vol. 1, 2002, pp. 320–326.
25. X. Hou and L. Zhang, "Saliency detection: A spectral residual approach," in *IEEE Computer Society Conference on Computer Vision and Pattern Recognition, CVPR 2007*, USA, June 2007, pp. 18–23.
26. E. J. Wood, "Applying fourier and associated transforms to pattern characterization in textiles," *Textile Research Journal*, vol. 60, no. 4, pp. 212–220, 1990.
27. S. Ying, G. Wu, Q. Wang, and D. Shen, "Hierarchical unbiased graph shrinkage (hugs): A novel groupwise registration for large data set," *NeuroImage*, vol. 84, pp. 626–638, 2014.
28. V. Navalpakkam and L. Itti, "An integrated model of top-down and bottom-up attention for optimizing detection speed," in *IEEE Computer Society Conference on Computer Vision and Pattern Recognition, CVPR 2006*, 2006, pp. 2049–2056.
29. M. Cheng, G. Zhang, N. J. Mitra, X. Huang, and S. Hu, "Global contrast based salient region detection," in *IEEE Conference on Computer Vision and Pattern Recognition, CVPR 2011*, 2011, pp. 409–416.
30. S. Goferman, L. Zelnik-Manor, and A. Tal, "Context-aware saliency detection," *IEEE Transactions on Pattern Analysis and Machine Intelligence*, vol. 34, no. 10, pp. 1915–1926, 2012.

31. J. Liu, P. Musialski, P. Wonka, and J. Ye, "Tensor completion for estimating missing values in visual data," *IEEE Transactions on Pattern Analysis and Machine Intelligence*, vol. 35, no. 1, pp. 208–220, 2013.
32. J. Liu, L. Yuan, and J. Ye, "An efficient algorithm for a class of fused lasso problems," in *Proceedings of the 16th International Conference on Knowledge Discovery and Data Mining*. Washington, DC, USA: ACM, July 2010, pp. 323–332.
33. G. Liu, Z. Lin, and Y. Yu, "Robust subspace segmentation by low-rank representation," in *Proceedings of the 27th International Conference on Machine Learning (ICML-10)*, Haifa, Israel, June 2010, pp. 663–670.
34. B. Cheng, G. Liu, J. Wang, Z. Huang, and S. Yan, "Multi-task low-rank affinity pursuit for image segmentation," in *IEEE International Conference on Computer Vision, 2011*, 2011, pp. 2439–2446.
35. C. Lang, G. Liu, J. Yu, and S. Yan, "Saliency detection by multitask sparsity pursuit," *IEEE Transactions on Image Processing*, vol. 21, no. 3, pp. 1327–1338, 2012.
36. Y. Yu and D. Schuurmans, "Rank/norm regularization with closed-form solutions: Application to subspace clustering," in *Proceedings of the Twenty-Seventh Conference on Uncertainty in Artificial Intelligence*, Barcelona, Spain, July 2011, pp. 778–785.
37. C. Lu, H. Min, Z. Zhao, L. Zhu, D. Huang, and S. Yan, "Robust and efficient subspace segmentation via least squares regression," in *12th European Conference on Computer Vision, ECCV 2012*, Florence, Italy, October 2012, pp. 347–360.
38. M. Varma and A. Zisserman, "A statistical approach to texture classification from single images," *International Journal of Computer Vision*, vol. 62, no. 1-2, pp. 61–81, 2005.
39. J. Cai, E. J. Candès, and Z. Shen, "A singular value thresholding algorithm for matrix completion," *SIAM Journal on Optimization*, vol. 20, no. 4, pp. 1956–1982, 2010.